

# Characterization of the NLRP1 inflammasome response in bovine species

Innate Immunity  
2020, Vol. 26(4) 301–311  
© The Author(s) 2019  
Article reuse guidelines:  
sagepub.com/journals-permissions  
DOI: 10.1177/1753425919886649  
journals.sagepub.com/home/ini  


Catherine E Vrentas<sup>1</sup> , Paola M Boggiatto<sup>1</sup>, Steven C Olsen<sup>1</sup>,  
Stephen H Leppla<sup>2</sup>  and Mahtab Moayeri<sup>2</sup>

## Abstract

Inflammasomes act as sensors of infection or damage to initiate immune responses. While extensively studied in rodents, understanding of livestock inflammasomes is limited. The NLRP1 inflammasome sensor in rodents is activated by *Toxoplasma gondii*, *Bacillus anthracis* lethal toxin (LT), and potentially other zoonotic pathogens. LT activates NLRP1 by N-terminal proteolysis, inducing macrophage pyroptosis and a pro-inflammatory cytokine response. In contrast, NLRP1 in macrophages from humans and certain rodent strains is resistant to LT cleavage, and pyroptosis is not induced. Evolution of NLRP1 sequences towards those leading to pyroptosis is of interest in understanding innate immune responses in different hosts. We characterized NLRP1 in cattle (*Bos taurus*) and American bison (*Bison bison*). Bovine NLRP1 is not cleaved by LT, and cattle and bison macrophages do not undergo toxin-induced pyroptosis. Additionally, we found a predicted *Nlrp1* splicing isoform in cattle macrophages lacking the N-terminal domain. Resistance to LT in bovine and human NLRP1 correlates with evolutionary sequence similarity to rodents. Consistent with LT-resistant rodents, bovine macrophages undergo a slower non-pyroptotic death in the presence of LPS and LT. Overall, our findings support the model that NLRP1 activation by LT requires N-terminal cleavage, and provide novel information on mechanisms underlying immune response diversity.

## Keywords

Bison, bovine, inflammasome, lethal toxin, NLRP1

Date Received: 26 May 2019; Revised 6 October 2019; accepted: 28 September 2019

## Introduction

Inflammasomes are cytosolic multiprotein assemblies that link signals of pathogen invasion or damage to associated host immune responses (reviewed by Broz and Dixit).<sup>1</sup> Classical inflammasome activation requires recognition of damage-associated molecular patterns (DAMPs) or PAMPs by PRRs, many of which are members of the NLR family. Formation of the inflammasome platform results in recruitment of pro-caspase-1, its subsequent cleavage into active caspase-1, and the maturation and secretion of IL-1 $\beta$  and IL-18. Active caspase-1 also cleaves gasdermin D, allowing for pore formation in the plasma membrane and the associated rapid lysis of cells, a process known as pyroptosis (“fiery death”; reviewed by Kovacs and Miao).<sup>2</sup> Well-studied inflammasomes include NLRP1,

NLRP3, NAIP-NLRC4, and AIM2, each sensing different danger signals.<sup>1</sup>

While the NLRP3 inflammasome is activated by a wide range of signals, including pore-forming bacterial toxins and crystalline material (reviewed by Broz and Dixit),<sup>1</sup> *Bacillus anthracis* lethal toxin (LT),<sup>3–6</sup> and the

<sup>1</sup>Infectious Bacterial Diseases Unit, National Animal Disease Center, Agricultural Research Service, US Department of Agriculture, Ames, USA

<sup>2</sup>Laboratory of Parasitic Diseases, National Institute of Allergy and Infectious Diseases, National Institutes of Health, Bethesda, USA

### Corresponding author:

Catherine E Vrentas, Infectious Bacterial Diseases Unit, National Animal Disease Center, Agricultural Research Service, US Department of Agriculture, Ames, IA 50010, USA.  
Email: cevrentas@gmail.com.



intracellular parasite *Toxoplasma gondii*,<sup>7-9</sup> are the two primary known activators of NLRP1. LT is a bipartite toxin consisting of protective antigen (PA) and lethal factor (LF). PA binds to cell surface receptors and oligomerizes to allow binding and transport of LF, a protease, into the cytosol of the host cell, where it can cleave NLRP1 and induce pyroptosis.<sup>10</sup>

The NLRP1 inflammasome response to LT is species- and strain-specific. In rodents, some strains express NLRP1 proteins that are sensitive to LT activation, and others express resistant variants and do not undergo pyroptosis in response to the toxin. LT cleaves the N-terminus of rodent NLRP1.<sup>4-6</sup> *Nlrp1b* alleles in mice encoding cleavage-sensitive proteins (*Nlrp1<sup>S/S</sup>*) are associated with protection from anthrax spore infection, suggesting a role for murine *Nlrp1b* in a protective immune response.<sup>11,12</sup>

The mechanism of NLRP1 activation by *T. gondii* is unknown, although reduction of cytosolic ATP (as a marker of energy stress) was suggested recently as a general mechanism of inflammasome activation.<sup>13,14</sup> A chemical mutagenesis screen recently identified three *Toxoplasma* dense granule proteins as mediators of NLRP1 activation.<sup>15</sup> Interestingly, while NLRP1 activation is responsible for rapid *T. gondii*-induced pyroptosis of macrophages in certain inbred rat strains, mouse macrophages from 12 tested inbred strains are resistant to pyroptosis by this parasite (M. Moayeri, unpublished observations).<sup>4,8</sup> In another paradox, NLRP1 sequence does not control murine organismal susceptibility to LT exposure, while rat organismal sensitivity to LT is correlated with NLRP1 sequence susceptibility to cleavage by the toxin. Some rats are highly sensitive to a rapid (1 h) vascular collapse upon LT injection.<sup>16</sup> Activation of NLRP1-mediated macrophage pyroptosis by LT in rats is perfectly correlated with, but does not directly contribute to, animal death (unpublished observations).

In contrast, while human macrophages express NLRP1, it is not cleaved by LT; therefore, humans do not appear to possess this sensing system to detect anthrax infection.<sup>17,18</sup> However, artificially induced cleavage of the N-terminus of human NLRP1 is sufficient to induce inflammasome activation.<sup>17</sup> Rodent NLRP1 proteins are distinct from human NLRP1 in that they do not contain the N-terminal pyrin domain involved in recruitment of the inflammasome scaffold protein ASC. Protein sequence analyses have led to the hypothesis that the N-terminus of NLRP1 in primates is evolving rapidly toward conservation of a cleavable N-terminal linker sequence, likely as a result of positive selection pressure from pathogen exposure.<sup>17</sup>

Recent findings suggest that the NLRP1 inflammasome may represent a more general sensing system for pathogen invasion, including sensing the presence of

intracellular microbes in macrophages. Neiman-Zenevich and colleagues demonstrated that *Listeria monocytogenes* and *Shigella flexneri*, both bacteria with an intracellular niche,<sup>14</sup> can also activate the NLRP1 inflammasome; the pyroptosis of cells harboring these microbes then exposes them to the immune system.<sup>19</sup> A recently developed unifying mechanism for NLRP1 activation suggests that proteasome-mediated degradation and release of the C-terminus of NLRP1 are both necessary and sufficient for NLRP1 activation.<sup>20,21</sup> This can occur subsequent to cleavage (LT) or to NLRP1 modifications by pathogen ubiquitin ligases (as in the case of activation by *Sh. flexneri*). Therefore, other pathogen factors with related activities may also serve as NLRP1 activators.

Despite the detailed characterization of inflammasome pathways in rodent and human systems, our understanding of inflammasome activation in livestock hosts of disease is limited (reviewed in Vrentas et al.).<sup>22</sup> Recently, the first characterization of NLRP3 activation in bovine cells was published,<sup>23</sup> but nothing is known of NLRP1 responses in these species, despite the fact that herbivores like cattle and bison, rather than rodents, are the most common hosts for anthrax in natural environments. Similarly, shedding of *Shigella* and *Listeria* from large ruminants is an important contributor to the environmental spread of these bacteria, which can also cause active disease in ruminants.<sup>24</sup> Characterization of NLRP1 responses in bovine species has the potential to reveal important species-related differences in immune responses, and may also be relevant to other intracellular pathogens, such as *Brucella* or *Mycobacteria*, which infect and cause disease in these species. Recently, the NLRP3 inflammasome has been demonstrated to be activated in response to *Brucella* infection, and pyroptosis and IL-18 production have been demonstrated to limit the spread of *Brucella* infection.<sup>25,26</sup>

In this study, we provide the first characterization of the NLRP1 inflammasome in cattle (*Bos taurus*) and American bison (*Bison bison*). Using LT as our model system for inflammasome activation, we characterize the response of primary bovine and bison macrophages to the toxin, assess cleavage of the N-terminus of bovine NLRP1 as compared with rat and human proteins, characterize the nature of the *NLRP1* transcripts produced in each organism, and discuss potential evolutionary relationships of NLRP1 across species.

## Materials and methods

### Proteins and reagents

Lethal factor (LF), the LF catalytic mutant E687C,<sup>27,28</sup> and PA were purified from non-pathogenic,

non-encapsulated (non-Select Agent) strains of *B. anthracis* at the National Institutes of Health as described by Park and Leppla.<sup>28</sup> Purified *Escherichia coli* LPS (O55:B5) was obtained from Sigma.

### **Bison and bovine monocyte-derived macrophages and mouse bone-marrow-derived macrophages**

Holstein cattle and American bison housed outside on the grounds of the National Animal Disease Center in Ames, Iowa, were sources of cells. All animal care and blood collection were performed under the guidance of the associated IACUC protocols at the National Animal Disease Center. Bovine and bison monocytes from uninfected/clean animals were prepared fresh from peripheral blood and were differentiated to macrophages via surface adhesion.

Venous blood ( $\approx 50$  ml/animal) was collected by venipuncture of steers into tubes containing acid-citrate-dextrose. To prepare PBMCs, the buffy coat was obtained by preparation over Ficoll 1077 (Sigma). Purified PBMCs were re-suspended in complete RPMI (Invitrogen; cRPMI) medium containing 10–20% FBS (GE Healthcare), 2 mM glutamine, 100 U penicillin/ml, 100  $\mu$ g streptomycin/ml, 25 mM HEPES, 1 mM sodium pyruvate, and 1 $\times$  essential and non-essential amino acids (Gibco, ThermoFisher) and plated at 37°C and 5% CO<sub>2</sub> in tissue culture-treated Petri dishes.

Adherent monocytes were allowed to differentiate into macrophages for  $\geq 7$  d before use in experiments. Macrophages were harvested by gentle scraping, and cell number was determined via hand counting on a hemocytometer and trypan blue exclusion. For all experiments, cell viability was confirmed to be  $> 90\%$ . Cell numbers were then adjusted depending on desired viable cell concentration.

Representative data from mouse macrophages was generated from bone-marrow-derived macrophages (BMDMs), using cells differentiated in conditioned L929 media for 7–9 d as described in Newman et al.<sup>29</sup> Collection of BMDMs was conducted under the relevant IACUC protocols at the National Institutes of Health.

### **Surface staining and CD14 flow cytometry**

CD14 expression analysis (Supplemental Figure 1c) was performed by flow cytometry using APC-labeled anti-human CD14 Ab and  $\approx 1 \times 10^6$  adherent cells. Cell viability was assessed by eF450 fixable viability dye (eBioscience) staining (1:1000, 20 min, 4°C). Nonspecific binding was blocked with Fc block (anti-CD16/CD32, 2.4G2; BD Biosciences) and 5% normal goat serum (EMD Millipore). Cells were incubated

with APC-labeled anti-human CD14 Ab (2  $\mu$ g per test; M5E2; BD Biosciences) or isotype control for 15 min on ice, washed twice with FACS buffer, re-suspended in stabilizing fixative (BD Biosciences) and data acquired on a LSRII flow cytometer (BD Bioscience). Data were analyzed using FlowJo software (FlowJo).

### **Cytotoxicity assays**

Monocyte-derived macrophages (MDM) seeded into 96-well plates were treated with LF (0–2  $\mu$ g/ml), PA (1  $\mu$ g/ml), and/or LPS (0.5  $\mu$ g/ml) for 4 or 16 h at 37°C before assessment of cell viability by MTT (3-(4,5-dimethylthiazol-2-yl)-2,5-diphenyltetrazolium bromide) assay. After toxin treatment, media was replaced for 2–4 h with phenol red-free cRPMI (Invitrogen/ThermoFisher) + 20% FBS containing 0.5 mg/ml MTT; MTT conversion was assessed via the manufacturer's kit protocol (Cayman Chemical, Ann Arbor, MI).

Experiments on MDMs were performed within 8–13 d of maturation post-collection of PBMCs. For experiments in Figure 1, adherent cells were removed by gentle scraping after 24 h (post-collection) and plated to  $5 \times 10^5$  cells/well in 96 well plates and stained by MTT after a medium change to remove non-adherent cells after  $> 7$  d (Figure 1). For experiments in Supplemental Figure 1c, media was changed after 24–48 h (post-collection), and cells were incubated an additional 7–10 d prior to replating at  $0.5\text{--}1 \times 10^5$  cells/well for MTT analysis. As displayed in Figure 1 and Supplemental Figure 1c (iv), cells prepared by each adherence/washing strategy were unresponsive to rapid cell death by LT.

### **MAPK Western blotting**

Bovine MDMs were plated to a 24-well tissue culture-treated plate ( $\approx 0.7 \times 10^6$  cells/well) and treated with LT (1  $\mu$ g/ml) for 4 h. RIPA buffer lysates were subjected to Western blot using rabbit anti-MAPK3 (Santa Cruz Biotech, Sc-959; 1:300) and/or rabbit anti-MAPK1 (US Biological, M2865-04B; 1:5000) primary Abs. Goat-anti-rabbit IR800CW secondary Ab (Licor; 1:20,000) was used for blot visualization on the Licor Odyssey system. LT-Treated or untreated lysates from mouse (Nlrp1<sup>S/S</sup>) BMDMs were run in parallel as positive controls for cleavage (data not shown).

### **Sequence information for generation of phylogenetic tree**

The following NCBI sequences were utilized to generate Figure 2a (all are NLRP1, unless indicated): bovine (*Bos taurus*), XP\_003587454; bison (*Bison bison*),

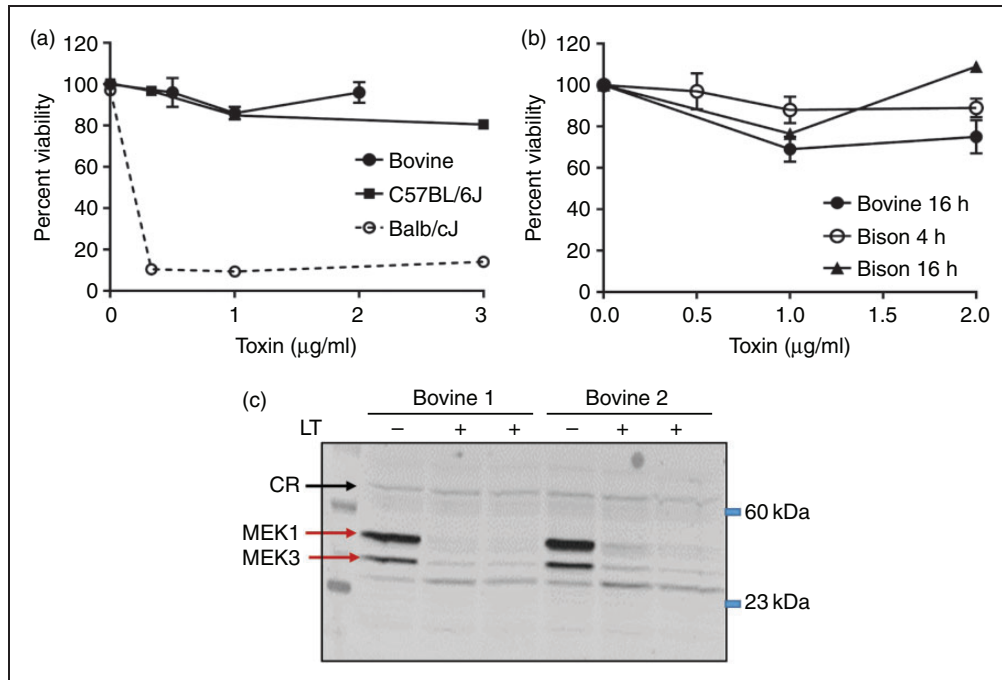


**Figure 1.** Response of bovine macrophages to LT. (a) Bovine macrophages obtained from four independent Holstein calves were incubated with LT (1  $\mu\text{g/ml}$  PA and 0–2.0  $\mu\text{g/ml}$  LF) for 4 h prior to assessment of cell viability. Individual data points represent the average of replicates at each concentration  $\pm$  SEM. Representative curves for LT treatment of BMDMs from *Nlrp<sup>R/R</sup>* (C57BL/6J) and *Nlrp<sup>S/S</sup>* (Balb/cJ) mice are shown for comparison. (b) Bison or bovine (Holstein cattle) macrophages were treated with LT (PA + LF) as described in (a) for either 4 h (bison, open circles) or 16 h (bovine, closed circles; bison, triangles) prior to assessment of viability by MTT assay. Data are averages for biological replicates of cells from between  $n = 2$  to  $n = 4$  individual animals at each time point, with error bars indicating SEM. (c) Western blot assessment of MAPK cleavage in lysates from LT-treated bovine MDMs (4 h, 1  $\mu\text{g/ml}$  LT). Lysates from two cattle (Bovine 1, Bovine 2) were examined. Blots were probed with anti-MAPK1 and re-probed with anti-MAPK3. “CR” indicates a cross-reactive band that serves as an equal loading control. Lysates from NLRP1-sensitive mouse macrophages were analyzed as a cleavage control.

XP\_010845734; dog (*Canis lupis familiaris*), XP\_005619937; human (*Homo sapiens*), NP\_127497; mouse (*Mus musculus*) NLRP1B isoform 1, NP\_001035786; mouse (*Mus musculus*) NLRP1B isoform 5, Q0GKD5; rat (*Rattus norvegicus*), NP\_001139227.2; and Bovine (*Bos taurus*) NLRP3, AAI47937.1.

#### Preparation of cattle cDNA and PCR amplification of bovine NLRP1 transcripts

Venous blood was collected from Holstein cattle at the National Animal Disease Center; RNA was extracted from whole white blood cells using the QIAamp RNA Blood Mini Kit (Qiagen) and converted into cDNA using the SuperScript III Reverse Transcriptase kit (ThermoFisher) following manufacturer’s instructions, using oligo(dT) priming. cDNA was used as a template for endpoint PCR reactions using primers CV1 (5'-CAGATTTGCTGAGATGCGGC-3') and CV4 (5'-AGGTGTCTCTCTCCTTTGATCCTG-3'), and the same primers were used for sequencing.

#### Expression and purification of GST-NLRP1 fusion proteins

GST-NLRP1 fusion proteins were overexpressed in *E. coli*. The rat construct (rat (1-100)) is described in Levinsohn et al.<sup>5</sup> and contains the first 100 amino acids of a cleavage-sensitive rat *Nlrp1* allele cloned C-terminally into the pEX-N-6HIS-GST vector. The bovine construct was synthesized by DNA2.0 (Newark, CA) and carries the (predicted) first 200 amino acids of the bovine variant X1 *Nlrp1* transcript cloned into a T7-GST vector, pD454-GST, C-terminally to the GST (bovine (1–200)). The human (1–201) and the bovine (151–250) construct were cloned (ATUM, Newark, CA) with a parallel scheme to the bovine (1–200) construct in pD454-GST.

Protein expression was induced in cultures of BL21 ( $\lambda$ DE3) carrying the desired expression plasmid by 1 mM IPTG addition for 3–4 h at 37°C. Proteins were purified from cell lysates (containing cOmplete protease inhibitor, ThermoFisher) by affinity chromatography over glutathione agarose (Pierce), with elution into 50 mM Tris-HCl pH 8.0 + 10 mM reduced glutathione.

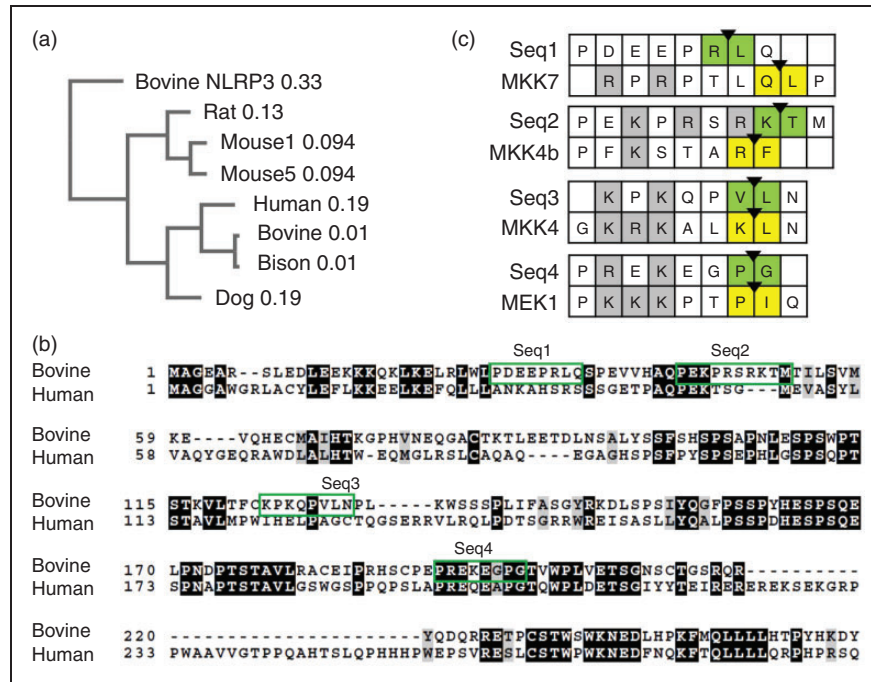


**Figure 2.** Analysis of bovine NLRP1 sequences. (a) Phylogenetic tree of NLRP1 sequences, derived from the NCBI nucleotide database; constructed via Clustal Omega using UPGMA methodology, with branch lengths indicated. Selected splice variants are indicated as different numbers (Mouse 1 vs Mouse 5). A bovine NLRP3 protein sequence is included as an outgroup. (b) Clustal Omega alignment of N-terminus of bovine NLRP1 predicted splice variant 1 (X1) and human NLRP1 splice variant 1, depicted using BOXSHADE. Green boxes depict potential cleavage sites for LF. (c) Alignment of potential bovine NLRP1 cleavage sites with known LF target sequences. Known MAPK cleavage sites from Vitale et al. were aligned with Clustal Omega to the four putative bovine NLRP1 cleavage sites.<sup>36</sup> Boxes compare each putative cleavage site with an aligning MAPK cleavage site (as determined from batch alignments and positioning of cleavage locations). MAPK cleavage sites have the position of peptide bond cleavage highlighted with an arrowhead, with flanking residues in yellow; NLRP1 putative sites have a potential cleavage site, based on positioning of a hydrophobic or similar residue in the 1' position (consistent with the consensus cleavage sequence), identified with an arrowhead and green highlighting.

Protein concentrations were measured by Bradford assay (Bio-Rad). Extensive dialysis into cleavage buffer was used to prevent inhibition of LF cleavage by residual glutathione.

Purified proteins were assessed by gel electrophoresis and Coomassie blue staining (Supplemental Figure 3c). Separation of rat, bovine, and human proteins were consistent with their expected sizes of 40, 49, and 49 kDa, respectively. The appearance of the rat construct was consistent with that in Levinsohn et al.,<sup>5</sup> including the presence of some breakdown products resulting from degradation by bacterial proteases during expression/purification. The bovine (151–250) product was extensively cleaved by cellular proteases (Supplemental Figure 3c), as the expected full-length size was 38 kDa.

### In vitro cleavage assays with lethal factor

GST-NLRP1 constructs were dialyzed into LF cleavage buffer (1  $\mu$ M ZnCl<sub>2</sub>, 5 mM NaCl, 10 mM HEPES) and incubated with either LF, a cleavage-defective LF

mutant (E687C), or no additional protein at 37°C for 3 h, as described in Levinsohn et al.<sup>5</sup> SDS-PAGE and either Coomassie blue staining or Western blotting with rabbit anti-GST Ab (Abcam, Cat. No. ab19256, 1:5000) was performed. Western detection was performed with secondary HRP-conjugated goat anti-rabbit Ab (KPL, Cat. No. 374-1506, 1:10,000), and chemiluminescent detection was performed with an ECL developer kit (Pierce ECL Western Blotting Substrate, Cat. No. 32106) and the ProteinSimple gel imager system.

## Results

### Bovine and bison monocyte-derived macrophages do not pyroptose in response to LT

LT-sensitive rodent BMDMs from mice that harbor *Nlrp1b*<sup>S/S</sup> alleles (such as BALB/cJ) undergo rapid pyroptotic death within 4 h of toxin treatment (Figure 1a, dashed line). We tested whether bovine blood MDM were similarly sensitive to LT. Rapid

lysis was not observed with LT concentrations as high as 2 µg/ml at 4 h (Figure 1a, closed circles), consistent with observations for pyroptosis-resistant macrophages from mouse strains harboring *Nlrp1<sup>R/R</sup>* alleles (C57BL/6J; Figure 1a, closed squares). We tested 12 different calves in the USDA National Animal Disease Center herd, and found the same resistance to rapid lysis (data not shown). A 20–30% reduction in viability was observed following overnight (ca. 16 h) treatment with LT (Figure 1b, closed circles; Supplemental Figures 1a–c), similar to levels of cell death observed in pyroptosis-resistant murine macrophages after 24–48 h of toxin treatment (representative data for two *Nlrp1<sup>R/R</sup>* strains, C57BL/6J and DBA/2J, is shown in Supplemental Figure 2a). Bison are evolutionarily closely related to cattle, so we hypothesized that bison MDMs would be similarly unresponsive to LT. Indeed, MDMs from American bison were also resistant to LT over 4–16 h of treatment (Figure 1b, open circles, closed triangles).

Resistance to a rapid pyroptosis-like cell death could be explained either by failure of LT to enter bovine MDMs due to low receptor numbers or other translocation issues, or, alternatively, by resistance of NLRP1 to cleavage by LF. We assessed cleavage of other cytosolic LT substrates – the MAPK proteins – in cattle macrophages after 4 h of LT treatment. Abs reactive to epitopes in the N-terminus of MAPK1 and MAPK3 were used to assess cleavage. The loss of the N-terminal region following cleavage by LT results in lack of reactivity with the Ab.<sup>30</sup> Nearly complete cleavage of both MAPK1 and MAPK3 was observed in treated MDMs from two different steers (Figure 1c), indicating that LF is rapidly translocated into and is active within the cytosol of bovine macrophages.

Previously, Park et al. and Kim et al. demonstrated that treatment of pyroptosis-resistant rodent macrophages with both LPS and LT led to sensitization to a slower (non-pyroptotic) cell death.<sup>31,32</sup> Park et al. described this effect as due to disruption of signaling pathways by LF cleavage in the presence of NF-κB activation.<sup>31</sup> Therefore, we tested whether activation of bovine MDMs with LPS would result in a similar slower cell death. While treatment with LPS alone did not cause cell death under these conditions (Supplemental Figure 2b), when bovine MDMs were simultaneously incubated with both LT and LPS overnight, we observed a reduction in cell viability as compared with LT alone at 16 h post-treatment (Supplemental Figure 2c).

### Comparison of bovine, human, and rodent NLRP1 genomic sequences

NLRP1 expression and the associated NLRP1 inflammasome have not previously been characterized

experimentally in bovine species. Previous work on rodent NLRP1 proteins suggests that the induction of pyroptosis by LT requires cleavage of the sensor's N-terminus. Therefore, we examined the cleavage model in the context of the sequence and biochemical properties of bovine NLRP1.

First, we characterized bovine *Nlrp1* expression patterns. Based on the *Bos taurus* “L1 Dominette” genome assembly (May 2018 annotation, NCBI reference sequence NC\_037346.1), multiple splice isoforms for the *Nlrp1* mRNA transcript and associated forms of the resulting NLRP1 protein are predicted *in silico* via NCBI's Gnomon analysis (with additional support from expressed sequence tag information).<sup>33</sup> When the predicted protein sequences (full-length variants) for bovine and bison NLRP1 are compared with the sequences of other mammalian NLRP1 proteins, they are more closely related to human and canine sequences than to rodent sequences (Figure 2a), consistent with the larger tree of NLRP sequences depicted in Tian et al.<sup>34</sup> Unsurprisingly, bison NLRP1 is closely related to the bovine sequence.

An NCBI search for bovine NLRP1 protein sequences reveals 11 different predicted splice variants based on the May 2018 annotation, some of which represent diversity in the N-terminal region. The 5' exon in bovine NLRP1 mRNA (452 nt) is non-protein coding; Exon 2 (corresponds to bovine NLRP1 residues #1–92) encodes the pyrin domain of bovine NLRP1, and it exhibits some homology to the human NLRP1 pyrin domain (Figure 2b). Exons 3, 4, and the first part of exon 5 comprise the linker between the PYD and the NBD (nucleotide-binding domain). Table 1 presents an overview of the composition of the N-terminus of each of the predicted bovine NLRP1 variants. Notably, multiple predicted splice isoforms are missing individual N-terminal exons, with the X8 variant predicted to be missing the entire N-terminus of the protein.

There is no well-defined sequence of amino acids recognized as the consensus LF cleavage site. LF cleavage sites in known substrates primarily share charge similarities, with up to eight basic or charged residues N-terminal to the cleavage site and a hydrophobic residue often found at the 1' position relative to the cleavage site.<sup>35</sup> Often, the region also has 2–4 proline residues in the region of basic or charged residues. Several potential LF cleavage sites were identified in the bovine NLRP1 N-terminus via sequence comparison to previously suggested LF cleavage motifs<sup>35–37</sup> in areas of significant variation between the bovine sequence and the uncleavable human NLRP1 sequence (green boxes in Figure 2b). The four potential cleavage sites identified through sequence gazing were aligned to known LF cleavage sites in MKK/MAPK proteins

**Table 1.** Summary of the composition of predicted bovine NLRP1 variants, based on NCBI computational predictions of *Nlrp1* splice sites. Shaded boxes indicate the presence of that exon in the variant; empty boxes indicate the absence of the exon in the variant for Exons 2–4. For the remainder of the protein (C-terminal sequences), notes are provided about the protein's composition.

Protein/splice variant	Exon 2 (pyrin domain)	Exon 3 (linker seq.)	Exon 4 (linker seq.)	Notes on C-terminal composition of the variant
	Residues 1–92	Residues 93–147	Residues 148–214	
X1				–
X2				Small internal deletion
X3				Matches X1
X4				Small internal deletion
X5				Matches X1
X6				Matches X1
X7				Deletion at C-terminal end
X8				Begins protein sequence at residue 244 in exon 5
X9				Predicted protein sequence fully matches X8 predicted sequence
X10				Predicted protein sequence fully matches X8 predicted sequence
X11				Deletion and variation at C-terminal end
X12				Protein sequence not predicted in NCBI annotation; annotated as misc_RNA

(Figure 2c). Alignments are not stringent due to the variable nature of the LF cleavage site across thus far identified target sites in different substrates within and across different species.

#### Characterization of bovine NLRP1 splicing isoforms

To examine the actual *Nlrp1* splicing isoforms that are present *in vivo* in cattle, we prepared RNA from bovine white blood cells obtained from four different cattle (Figure 3a, i) and sequenced *Nlrp1* mRNA transcripts, utilizing primers that anneal to exon 1 and exon 5 of the predicted transcript to amplify the 5' region (encoding the N-terminus of the bovine NLRP1 protein). Using oligo(dT)-primed cDNA as a template, a series of bands were obtained for each animal (Figure 3a, ii). The sequence of Band A matched that of variant X1 (as well as the other variants with intact N-termini; X1 is the predicted full-length mRNA transcript). Interestingly, Band B represented a splice variant with exon 1 fused directly to exon 5 (Figure 3a, ii). Since exon 1 is noncoding, the product in Band B would need to utilize a separate ATG codon as a start site to be translated, and the resulting product would not include the pyrin domain. Therefore, Band B is consistent with predicted variant X8 (Table 1) and indicates that *Nlrp1* mRNA lacking this pyrin and linker domain region is indeed produced in appreciable levels in bovine macrophages. PCR products of intermediate size are expected to reflect alternative splicing combinations of exons 2, 3, and 4 [Figure 3a (ii),

asterisks], which would correspond to predicted variants X3, X5, and X6 (Table 1), and possibly other combinations.

#### Testing LF cleavage of bovine NLRP1

A recent study by Chavarria-Smith et al. found evidence that the sequence of the N-terminal NLRP1 linker region between the PYD and NBD domains is undergoing positive selection, driving variations across species towards LF-cleavable sequences.<sup>17</sup> The authors identified positive selection sites in the linker region between human NLRP1 residues 187 and 213. We examined this region in other even-toed ungulate species, compared with the human NLRP1 sequence as a reference. Residues that exhibited variation/polymorphism in the human *vs* New World monkey sequences, as demonstrated by Chavarria-Smith et al.,<sup>17</sup> are highlighted in blue (Supplemental Figure 3a). Although bovine NLRP1 is more similar to non-cleavable human NLRP1 than to LT-sensitive rodent variants, there is significant sequence divergence in this region in the human *vs* bovine sequences, as well as significant sequence divergence across even-toed ungulates. Therefore, despite the resistance of human NLRP1 to LF cleavage, there is potential for existence of cleavable sequences in bovine NLRP1s. Furthermore, because certain murine inbred strains such as NOD/LtJ have perfect LF cleavage sites but remain resistant to activation by the toxin due to other sequence polymorphisms,<sup>4,38</sup> we hypothesized that it was possible that

LT cleaves bovine NLRP1, but that resistance to inflammasome activation and rapid cell death is due to unknown polymorphisms elsewhere in the sensor. Therefore, we examined the cleavage susceptibility of the N-terminus of bovine NLRP1 to LF.

A protein construct consisting of the first 100 amino acids (aa) of (cleavage-sensitive) rat NLRP1 fused C-terminally to GST [denoted as rat(1-100)] could be cleaved by LF.<sup>5</sup> We prepared protein from both the same rat construct and a similar construct expressing the first 200 amino acids of bovine NLRP1 (full-length splice variant) fused to GST. The rationale for using the larger construct for bovine NLRP1 was to ensure that no cleavage sites for LF were missed in the N-terminus, and to include the most promising potential cleavage site (sequence 3), which starts at amino acid 123. The 200-amino acid sequence extends up until the endpoint of the fourth potential cleavage site (sequence 4) described above.

Purified rat (1-100) and bovine (1-200) GST-NLRP1 fusion proteins were characterized by Western blotting with anti-GST Ab. In the presence of zinc and a 3.6:1 ratio of GST-NLRP1: LF, the rat(1-100) construct was cleaved by LF, but not by an enzymatically inactive LF mutant (E687C, Figure 3b), to liberate a smaller cleavage product visible by Coomassie staining (Supplemental Figure 3b, red arrow). In contrast, no changes in migration of GST-reactive proteins were observed for the bovine (1-200) construct after LF treatment (Figure 3b, "LF" lanes; Supplemental Figure 3b). Additionally, there was no banding difference for the bovine (1-200) construct following cleavage with proteolytically active LF vs mutant LF [Figure 3b, "LF" vs "LF(E687C)"]. Similar to the bovine (1-200) construct, a purified GST-human NLRP1 (aa 1-201) construct [human (1-201)] was resistant to LF cleavage (Figure 3c). The presence of the human (1-201) protein did not block rat (1-100) cleavage, confirming that the lack of cleavage is not

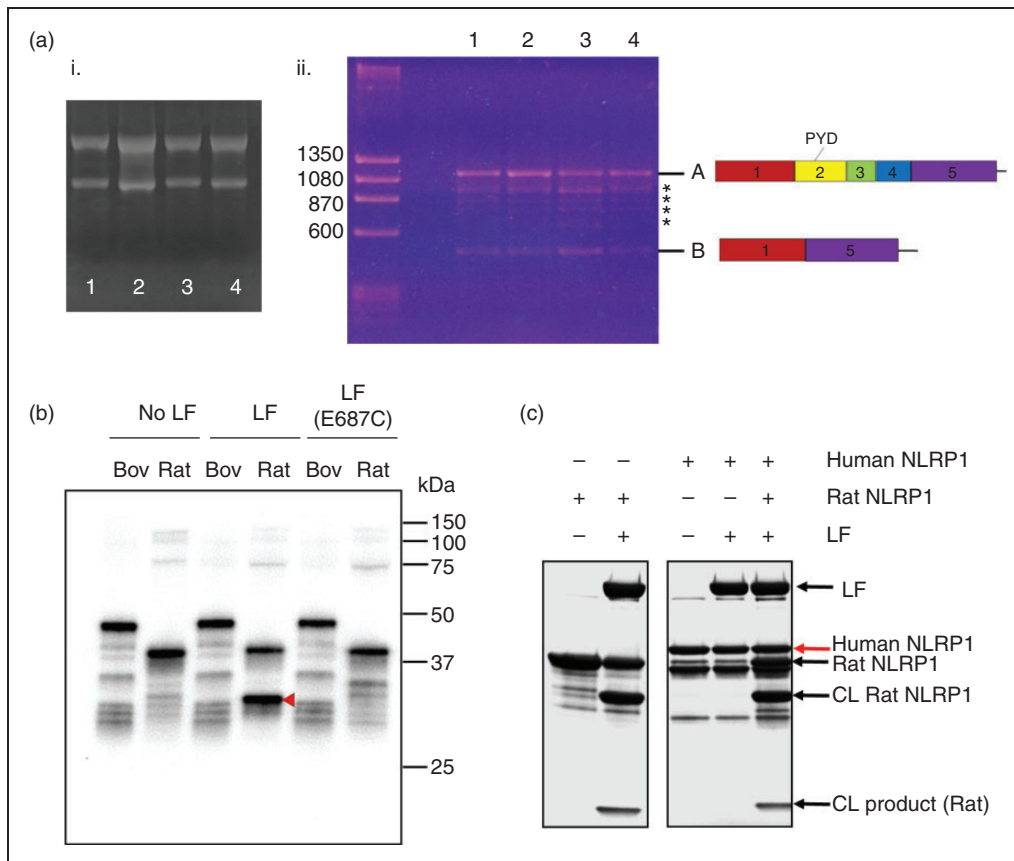


**Figure 3.** mRNA and protein analysis for bovine NLRP1. (a) PCR products generated from bovine *Nlrp1* transcript amplification. (i) Profiles of whole RNA isolated from four individual Holstein cattle (#1-4) (ii) PCR reactions using primers CV1 and CV4, with cDNA from cattle #1-4. Ladder band sizes are shown in base pairs. Diagrams of the N-termini of *Nlrp1* transcripts are depicted to the right of Bands A and B; intermediate-sized bands are indicated with asterisks. (b) Western blot (anti-GST Ab) of LF cleavage of bovine (1-200) and rat (1-100) GST-NLRP1 proteins. (c) Coomassie stained gel of human (1-201) GST-NLRP1 LF cleavage reactions, as described in (b), including reactions in which equal volumes of human (1-201) and rat (1-100; LF-sensitive) GST-NLRP1 were mixed prior to digestion. Constructs indicated as "NLRP1" are GST-NLRP1 fusions as described in materials and methods. "CL" = Cleaved rat (1-100) GST-NLRP1; "CL product" = cleavage product from LF-treated rat (1-100) GST-NLRP1.



due to inhibitory components in the uncleavable protein preparations (Figure 3c). The same result was also observed when mixing bovine and rat proteins (data not shown).

## Discussion and conclusions

The rodent NLRP1 inflammasome is activated by proteolytic cleavage.<sup>4–6,17</sup> Recent work on NLRP1 in human macrophages is suggestive of positive selection at the allele in the linker sequence of the N-terminus in primates, which is proposed to be related to selection pressure due to exposure to infections like anthrax.<sup>17</sup> Before this report, little was known about the role of the NLRP1 inflammasome in natural host species of anthrax, such as even-toed ungulates like cattle (*Bos taurus*) and American bison (*Bison bison*). Here, we demonstrate that, consistent with its evolutionary similarity to human (vs. rodent) NLRP1, the bovine NLRP1 sequence is not susceptible to cleavage by LF, and that both bovine and bison macrophages are resistant to toxin-induced rapid cell death. The lack of observable cleavage is consistent with the model that resistance to LT-induced pyroptosis is correlated with the inability of the toxin to cleave NLRP1 in a strain- and species-dependent manner. Bovine macrophages do, however, undergo cell death over a longer time frame, consistent with the apoptotic death seen in macrophages and dendritic cells from rodents carrying *Nlrp1*<sup>R/R</sup> alleles (and expressing uncleavable NLRP1 proteins). LF is able to enter the bovine macrophage to cleave MAPKs, which may contribute to this non-pyroptotic cell death.

In addition to providing further support for the cleavage requirement for NLRP1 inflammasome activation in response to LT, these findings bring into question the idea that mammalian NLRP1 sequences are evolving in response to pressure due to infection with *B. anthracis*. Presumably, natural hosts like cattle and bison would be under some of the strongest pressure for sequence selection towards a pyroptotic response to LT if this response, and the pro-inflammatory consequences of inflammasome activation, are protective against spore infection. The lack of this response suggests that positive selection in cattle, bison, primates and other species may be related to another source of disease pressure. The response to *T. gondii*, which readily infects humans worldwide, could be an alternative source of this selective pressure. Additionally, the expanding information about the role of intracellular bacterial pathogens in NLRP1 activation suggests that evolution could be in response to other pathogens,<sup>14,20</sup> and/or to a more generic/promiscuous mechanism of activation, such as intracellular ATP stress. Alternatively, the absence of the cleavage event may have unknown beneficial effects in the primate or bovine hosts during bacterial infections, independent of

control of the innate immune response, providing a stronger evolutionary pressure in these hosts. We also note that the cattle used in this study were all of the Holstein breed and derived from Iowa herds. It remains a possibility that there is sequence divergence that leads to NLRP1 cleavage in some genetically distinct bovine populations.

Of note are the properties of a second construct attempted in this study, fusing the bovine NLRP1 sequence (aa 151–250) to GST [denoted as bovine (151–250)]. The main bovine (1–200) construct characterized here was designed to correspond with the previously published rat construct, with the NLRP1 sequence cloned C-terminally to the GST protein. This construction places the region of sequence divergence identified by Chavarria-Smith et al., as well as putative cleavage sequence 4, at the C-terminus of the purified protein, and cleavage may not be efficient in this construct and/or may not be discernable by electrophoresis.<sup>17</sup> Therefore, a separate bovine (151–250) construct was purified in an attempt to further examine LF cleavage in this region. This construct was highly susceptible to autoproteolysis during recombinant protein purification (Supplemental Figure 3c), precluding additional characterization of potential cleavage sites within this region. However, these results also suggest that this region of the protein is naturally sensitive to cleavage by proteases. Indeed, the region from amino acids ≈90–210 in human NLRP1 is predicted to lack secondary structure,<sup>17</sup> and the same is true for the bovine NLRP1 sequence (Supplemental Figure 4). Engineering of artificial cleavage sites into this region of human NLRP1 was sufficient for removal of the pyrin domain and subsequent NLRP1 activation.<sup>17</sup> It was suggested that this unstructured region could be a target for inflammasome activation by diverse bacterial proteases. The results for the bovine (151–250) protein are consistent with this possibility.

Finally, the presence of a bovine *Nlrp1* splicing isoform missing the entirety of the exons encoding the N-terminus is notable in the bovine system. The potential role of this variant in bovine inflammatory mechanisms is unknown, but of potential future interest to comparative immunology. As it is possible that the truncated transcript is not translated into functional protein, the presence of stable protein representing different isoforms would need to be confirmed.

Overall, the work presented here provides the first characterization of the NLRP1 inflammasome in bovine species and demonstrates the utility of expanding our understanding of innate immune mechanisms to species beyond rodent models, especially in the case of zoonotic infections with livestock and/or wildlife hosts. While current knowledge of the role of the inflammasome in livestock vectors of disease is still

limited, there is an expanding literature on the impact of the NLRP3 inflammasome in multiple livestock species, especially swine (reviewed in Vrentas et al.).<sup>22</sup> Expansion of our characterization of inflammasomes in bovine species has the potential to contribute to our understanding of differences between either bovine and human, or bovine and wildlife, species in terms of susceptibility to zoonotic infections, differences in disease virulence and persistence, and/or differences in vaccine responses.

### Acknowledgments

The authors thank Lilia Walther for her expert technical assistance, the animal care and veterinary staff at the National Animal Disease Center, and Rasem Fattah for assistance in purifying proteins.

### Declaration of conflicting interests


The author(s) declared no potential conflicts of interest with respect to the research, authorship, and/or publication of this article.

### Funding

The author(s) disclosed receipt of the following financial support for the research, authorship, and/or publication of this article: This manuscript was supported by the intramural program of the National Institute of Allergy and Infectious Disease, National Institutes of Health; and the intramural funds of the Agricultural Research Service, United States Department of Agriculture (USDA). Disclaimer: Mention of trade names or commercial products in this article is solely for the purpose of providing specific information and does not imply recommendation or endorsement by the USDA. USDA is an equal opportunity employer.

### ORCID iDs

Catherine E Vrentas  <https://orcid.org/0000-0003-1434-654X>

Stephen H Leppla  <https://orcid.org/0000-0001-5233-0501>

### Supplemental material

Supplemental material for this article is available online.

### References

1. Broz P, Dixit VM. Inflammasomes: mechanism of assembly, regulation and signalling. *Nat Rev Immunol* 2016; 16: 407–420.
2. Kovacs SB, Miao EA. Gasdermins: Effectors of pyroptosis. *Trends Cell Biol* 2017; 27: 673–684.
3. Boyden ED, Dietrich WF. Nalp1b controls mouse macrophage susceptibility to anthrax lethal toxin. *Nat Genetics* 2006; 38: 240–244.
4. Hellmich KA, Levinsohn JL, Fattah R, et al. Anthrax lethal factor cleaves mouse Nlrp1b in both toxin-sensitive and toxin-resistant macrophages. *PLoS One* 2012; 7: e49741.
5. Levinsohn JL, Newman ZL, Hellmich KA, et al. Anthrax lethal factor cleavage of Nlrp1 is required for activation of the inflammasome. *PLoS Pathog* 2012; 8: e1002638.
6. Chavarría-Smith J, Vance RE. Direct proteolytic cleavage of NLRP1 is necessary and sufficient for inflammasome activation by anthrax lethal factor. *PLoS Pathog* 2013; 9: e1003452.
7. Cavailles P, Flori P, Papapietro O, et al. A highly conserved Toxo1 haplotype directs resistance to toxoplasmosis and its associated caspase-1 dependent killing of parasite and host macrophage. *PLoS Pathog* 2014; 10: e1004005.
8. Cirelli KM, Gofu G, Hassan MA, et al. Inflammasome sensor NLRP1 controls rat macrophage susceptibility to *Toxoplasma gondii*. *PLoS Pathog* 2014; 10: e1003927.
9. Ewald SE, Chavarria-Smith J, Boothroyd JC. NLRP1 is an inflammasome sensor for *Toxoplasma gondii*. *Infect Immun* 2014; 82: 460–468.
10. Moayeri M, Leppla SH, Vrentas C, et al. Anthrax pathogenesis. *Annu Rev Microbiol* 2015; 69: 185–208.
11. Moayeri M, Crown D, Newman ZL, et al. Inflammasome sensor Nlrp1b-dependent resistance to anthrax is mediated by caspase-1, IL-1 signaling and neutrophil recruitment. *PLoS Pathog* 2010; 6: e1001222.
12. Terra JK, Cote CK, France B, et al. Resistance to *Bacillus anthracis* infection mediated by a lethal toxin sensitive allele of Nalp1b/Nlrp1b. *J Immunol* 2010; 184: 17–20.
13. Liao KC, Mogridge J. Activation of the Nlrp1b inflammasome by reduction of cytosolic ATP. *Infect Immun* 2013; 81: 570–579.
14. Neiman-Zenevich J, Stuart S, Abdel-Nour M, et al. *Listeria monocytogenes* and *Shigella flexneri* activate the NLRP1B inflammasome. *Infect Immun* 2017; 85: 11.
15. Wang Y, Cirelli KM, Barros PDC, et al. Three *Toxoplasma gondii* dense granule proteins are required for induction of Lewis rat macrophage pyroptosis. *mBio* 2019; 10: e02388-18.
16. Newman ZL, Printz MP, Liu S, et al. Susceptibility to anthrax lethal toxin-induced rat death is controlled by a single chromosome 10 locus that includes rNlrp1. *PLoS Pathog* 2010; 6: e1000906.
17. Chavarría-Smith J, Mitchell PS, Ho AM, et al. Functional and evolutionary analyses identify proteolysis as a general mechanism for NLRP1 inflammasome activation. *PLoS Pathog* 2016; 12: e1006052.
18. Moayeri M, Sastalla I, Leppla SH. Anthrax and the inflammasome. *Microbes Infect* 2012; 14: 392–400.
19. Jorgensen I, Miao EA. Pyroptotic cell death defends against intracellular pathogens. *Immunol Rev* 2015; 265: 130–142.
20. Sandstrom A, Mitchell PS, Goers L, et al. Functional degradation: A mechanism of NLRP1 inflammasome activation by diverse pathogen enzymes. *Science* 2019; 364: pii: eaau1330.
21. Chui AJ, Okondo MC, Rao SD, Gai K, Griswold AR, et al. N-terminal degradation activates the NLRP1B inflammasome. *Science* 2019; 364: 82–85.

22. Vrentas CE, Schaut RG, Boggiatto PM, et al. Inflammasomes in livestock and wildlife: Insights into the intersection of pathogens and natural host species. *Vet Immunol Immunopathol* 2018; 201: 49–56.
23. Harte C, Gorman AL, McCluskey S, et al. Alum activates the bovine NLRP3 inflammasome. *Front Immunol* 2017; 9: 1494.
24. McDaniel CJ, Cardwell DM, Moeller RB, et al. Humans and cattle: A review of bovine zoonoses. *Vector Borne Zoonotic Dis* 2014; 14: 1–19.
25. Marim FM, Franco MMC, Gomes MTR, et al. The role of NLRP3 and AIM2 in inflammasome activation during *Brucella abortus* infection. *Semin Immunopathol* 2017; 39: 215–223.
26. Lacey CA, Mitchell WJ, et al. Caspases-1 and caspase-11 mediate pyroptosis, inflammation, and control of *Brucella* joint infection. *Infect Immun* 2018; 86: pii: e00361-18.
27. Klimpel KR, Arora D, Leppla SH. Anthrax toxin lethal factor contains a zinc metalloprotease consensus sequence which is required for lethal toxin activity. *Mol Microbiol* 1994; 13: 1093–1100.
28. Park S, Leppla SH. Optimized production and purification of *Bacillus anthracis* lethal factor. *Protein Expr Purif* 2000; 18: 293–302.
29. Newman ZL, Crown D, Leppla SH, et al. Anthrax lethal toxin activates the inflammasome in sensitive rat macrophages. *Biochem Biophys Res Commun* 2010; 398: 785–789.
30. Greaney AJ, Maier NK, Leppla SH, et al. Sulforaphane inhibits multiple inflammasomes through an Nrf2-independent mechanism. *J Leukoc Biol* 2016; 99: 189–199.
31. Park JM, Greten FR, Li ZW, et al. Macrophage apoptosis by anthrax lethal factor through p38 MAP kinase inhibition. *Science* 2002; 297: 2048–2051.
32. Kim SO, Jing Q, Hoebe K, et al. Sensitizing anthrax lethal toxin-resistant macrophages to lethal toxin-induced killing by tumor necrosis factor- $\alpha$ . *J Biol Chem* 2003; 278: 7413–7421.
33. Zimin AV, Delcher AL, Florea L, et al. A whole genome assembly of the domestic cow, *Bos taurus*. *Genome Biol* 2009; 10: R42.
34. Tian X, Pascal G, Monget P. Evolution and functional divergence of *NLRP* genes in mammalian reproductive systems. *BMC Evol Biol* 2009; 9: 202.
35. Turk BE, Wong TY, Schwarzenbacher R, et al. The structural basis for substrate and inhibitor selectivity of the anthrax lethal factor. *Nat Struct Mol Biol* 2004; 11: 60–66.
36. Vitale G, Bernardi L, Napolitani G, et al. Susceptibility of mitogen-activated protein kinase family members to proteolysis by anthrax lethal factor. *Biochem J* 2000; 352: 739–745.
37. Chopra AP, Boone SA, et al. Anthrax lethal factor proteolysis and inactivation of MAP-kinase-kinase. *J Biol Chem* 2003; 278: 9402–9406.
38. Frew BC, Joag VR, Mogridge J. Proteolytic processing of Nlrp1b is required for inflammasome activity. *PLoS Pathog* 2012; 8: e1002659.